# Semi-analytic subsidence prediction

P. A. Fokker
*Netherlands Institute of Applied Geoscience TNO*

## Abstract

Subsidence of the surface due to the extraction of gas or oil from hydrocarbon reservoirs can in some cases be considerable. Two places where this is a problem are the Groningen field in The Netherlands and the Ekofisk field offshore Norway. Two approaches have traditionally been used to calculate subsidence: analytical and numerical. This paper presents a semi-analytical method, which has broader applicability than analytical models while calculation times remain very short. This new method can be applied for a multilayer subsurface in which the elastic properties vary per layer. It performed excellently in a validation exercise against analytical and numerical approaches. Further, the flexibility of the method was demonstrated using a field case. The new approach does not yet incorporate the viscoelastic behaviour of salt layers; this is scheduled for the near future.

## 1 Introduction

The extraction of gas or oil from a hydrocarbon reservoir causes changes in the stresses and strains due to the reduction in pore pressure. The resulting compaction may cause subsidence of the surface that can sometimes be considerable. Two places where this is a problem are the Groningen gas field in the Netherlands [1] and the Ekofisk field in the Norwegian sector of the North Sea [2].

Two approaches have traditionally been used to calculate subsidence for a given compaction: analytical and numerical. Use of existing analytical methods, though, is restricted to one or two homogeneous layers. The Geertsma method, for example, is limited to homogeneous subsurface properties [3], [4], [5]. Numerical approaches, on the other hand, may be comprehensive but are not always suited to quick sensitivity calculations or scenario evaluations. An example of a numerical model is DIANA, a finite-element simulator for elasticity calculations [6]. This paper presents a method that

combines elements of both approaches. It is similar to Boundary-Element methods [7]; the method combines a number of analytic functions that satisfy the elasticity equations in such a way that the boundary conditions are approximated. Such an approach makes the method broader applicable than analytical approaches, while the calculation times are much smaller than for finite-element simulators. The difference with conventional Boundary Element Methods is that we take singularities outside the domain, rather than distributed singularities on the boundary. Further, we use a least-squares approach to approximate the boundary conditions rather than the conventional approach which fulfils the boundary conditions exactly in a number of points, equal to the number of free parameters in the solution of the elasticity equations.

The new method starts from a given reservoir compaction and aims at the prediction of the displacement field at the surface. First, the effect of the volume decrease due to a localized centre of compression is modeled by evaluating the effect of a nucleus of strain at the depth of the reservoir. The resulting field is used as a Green function for integration over the reservoir to evaluate the full subsidence bowl. The new method can be applied for a multi-layer subsurface in which the elastic properties vary per layer.

As a first validation it has been checked whether, in the case of a single layer, the results reproduce Geertsma's formula; for an additional underlying basement with infinite rigidity, the rigid basement results should be regained. In addition, the new method has, for a multi-layer model, more thoroughly been validated against DIANA, a finite-element simulator. The new method performs excellently. Further, the flexibility of the method is demonstrated in a field case.

## 2 Definitions

The two relevant equations in the theory of linear elasticity, including poro-elastic effects, are Hooke's law and the equilibrium equation [3] (taking compressive stresses and strains negative):

$$\sigma_{ij} = 2G\varepsilon_{ij} + \left[\frac{2G\nu}{1-2\nu}\varepsilon_{kk} - \alpha_{\text{Biot}}\Delta p\right]\delta_{ij} \tag{1}$$

$$\partial_j \sigma_{ij} = 0 \tag{2}$$

in which $G$ and $\nu$ are the shear modulus and the Poisson ratio; $\alpha_{\text{Biot}}$ is the Biot constant [8]. The description of poro-elasticity and thermo-elasticity is analogous; for the analogy, $\alpha_{\text{Biot}}\Delta p$ must be identified with $2G\frac{1+\nu}{1-2\nu}\alpha_T\Delta T$, in which $\alpha_T$ is the thermal expansion coefficient.

Media with piecemeal homogeneous elasticity parameters are treated. The boundary conditions for such systems consist of vanishing tractions at the surface, and continuous tractions and displacements ($u_i$) at interfaces. For parallel layers with the interface perpendicular to the $z$-axis, the tractions at the interfaces are denoted by $\sigma_{i3}$.

Solutions to these equations can be conveniently formulated using potential functions; we use Galerkin stress functions [9]. With a Galerkin vector $\mathbf{F}$ the displacements and the stresses are given by

$$u_i = \frac{1}{2G}\left\{2\left[1-\nu\right]\nabla^2 F_i - \partial_i\partial_k F_k\right\} \tag{3}$$

$$\sigma_{ij} = \left(\nu\delta_{ij}\nabla^2 - \partial_i\partial_j\right)\partial_k F_k + \left[1-\nu\right]\nabla^2\left(\partial_i F_j + \partial_j F_i\right) \tag{4}$$

The present study makes frequent use of nuclei of strain. A nucleus of strain is a well-defined singularity, for instance a finite force working on a single point. A centre of compression is a nucleus of strain as well. Locating such nuclei at $(0,0,z_n)$ ($n$ being a counter for different possible positions) and directing them along the $z$-axis, the following Galerkin stress vectors are associated with a single force, a double force, a centre of compression, and a centre of compression dipole, for a homogeneous, unlimited medium ($\mathbf{k}$ is the unit vector in the $z$ direction and $R_n = \sqrt{x^2+y^2+(z-z_n)^2}$):

$$\mathbf{F}_{\text{single force}} = \mathbf{k}A_n R_n \tag{5}$$

$$\mathbf{F}_{\text{double force}} = \mathbf{k}B_n\frac{z-z_n}{R_n} \tag{6}$$

$$\mathbf{F}_{\text{centre of compression}} = \mathbf{k}E_n\log\left(R_n+z-z_n\right) \tag{7}$$

$$\mathbf{F}_{\text{dipole}} = \mathbf{k}H_n\frac{1}{R_n} \tag{8}$$

The constants $A$, $B$, $E$ and $H$ are the strengths of the associated nuclei. For a volume $\delta V$ which is reduced in pressure by an amount $dP$, the strength $E_0$ is given by

$$E_0 = -\alpha_{\text{Biot}}\frac{1-2\nu}{1-\nu}\frac{\delta V\,dP}{4\pi} = -2G\,C_m\frac{\delta V\,dP}{4\pi} \tag{9}$$

in which the correlation $C_m = \alpha_{\text{Biot}}\frac{1-2\nu}{2G(1-\nu)}$ has been used for the compaction coefficient $C_m$.

## 3 Statement of the new method

The new method starts with the solution of the elasticity equations around a centre of compression in the unlimited 3-dimensional space, in the form of its Galerkin stress function, Eq. 7. The centre of compaction is used to represent the compacting reservoir, and the solution around it would be the full solution in case of an infinite space with homogeneous properties: it is appropriate at the cause of the field, i.e. at the compacting reservoir, and it vanishes at infinity as it should. The other boundary conditions however, at the surface and at the interfaces, are not fulfilled with this basic solution

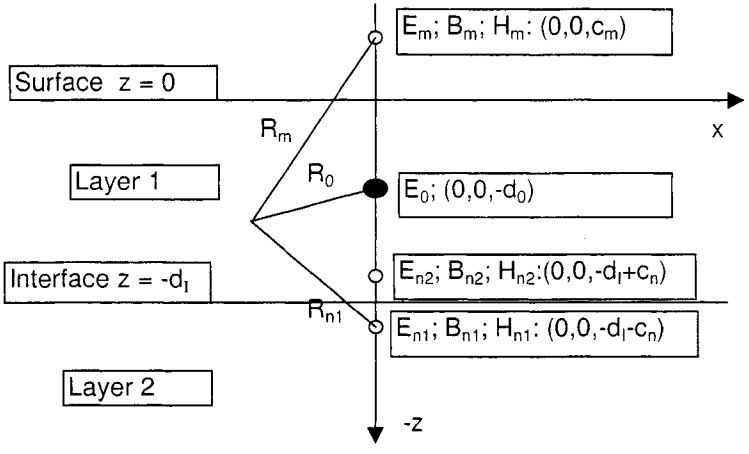



Figure 1: Schematic representation of the nuclei of strain: The stress- and strain field of the center of compression, $E_0$ at $(0, 0, -d)$, and of the fictitious nuclei of strain at $(0, 0, c_m)$ apply in both layers; the fields of the fictitious nuclei at $(0, 0, -d_I - c_n)$ and at $(0, 0, -d_I + c_n)$ apply in layers 1 and 2, respectively.

only: the fields derived from the stress functions depend on $G$ and $\nu$ and are therefore not continuous across elasticity interfaces. The solution around the centre of compaction is therefore complemented by other solutions to the elasticity equations. The additional solutions contain free parameters which are adjusted to approximate the boundary conditions, viz. continuity of displacements and of tractions at interfaces and zero tractions at the surface. The best approximation is achieved by minimising the summated squared deviation from the zero traction or the zero difference.

The additional solutions are taken as originating from fictitious nuclei of strain. A number of these nuclei are positioned around an interface. The field of a nucleus above the interface is applied only below the interface, and vice versa. This way the singularity is kept outside the domain of application of the elastic field and the solution is a real solution to the elasticity equations in the full application domain. (Fig. 1). The piecemeal application of additional fields induces additional discontinuities in the tractions and the displacements that can be influenced and optimised, to meet the boundary conditions, by adjusting the strength of the nuclei causing it. Clearly, nuclei close to the interface act rather locally, while those further away have a more global influence. A similar concept was used by Fitts for the calculation of the flow field in a porous medium [10].

For the fictitious nuclei of strain we take combinations of centres of compression or dilatation, and double forces and doublets of centres of com-

pression in the $z$-direction. We have experienced that this generally gives sufficient flexibility for problems with circular symmetry around the $z$-axis. The resulting Galerkin stress vector function in the two layers are given by

$$\begin{aligned}
\mathbf{F}^1 &= \mathbf{k}E_0 \log(R_0 + z + d_0) \\
&+ \mathbf{k}\sum_{n1}\left[E_{n1}\log(R_{n1} + z + d_I + c_{n1}) + B_{n1}\frac{z + d_I + c_{n1}}{R_{n1}} + \frac{H_{n1}}{R_{n1}}\right] \\
&+ \mathbf{k}\sum_{m}\left[E_m \log(R_m + z - c_m) + B_m\frac{z - c_m}{R_m} + \frac{H_m}{R_m}\right] \qquad (10) \\
\mathbf{F}^2 &= \mathbf{k}E_0 \log(R_0 + z + d_0) \\
&+ \mathbf{k}\sum_{n2}\left[E_{n2}\log(R_{n2} + z + d_I - c_{n2}) + B_{n2}\frac{z + d_I - c_{n2}}{R_{n2}} + \frac{H_{n2}}{R_{n2}}\right] \\
&+ \mathbf{k}\sum_{m}\left[E_m \log(R_m + z - c_m) + B_m\frac{z - c_m}{R_m} + \frac{H_m}{R_m}\right] \qquad (11)
\end{aligned}$$

The setup of Fig. 1 is straightforwardly extended to a multi-layer setup: the fields of the $n_2$ nuclei are applied at all positions below the interface with which it is connected, across lower lying interfaces. Similarly, the field of the $n_1$ nuclei are applied at all positions above the interface.

The resulting solution is the subsidence bowl of a centre of compression, the latter being a mathematical representation of an amount of compaction concentrated in a single point. This solution is then used as a kind of Green function in conjunction with the reservoir geometry to arrive at the subsidence bowl for the reservoir under compaction; an integration is made by varying the origin and strength of the symmetrical nucleus-of-strain solution over the position in the reservoir.

## 4 Validation

The new method has been compared with existing analytical and numerical packages. Figure 2 presents the elasticity profile of a two-layer system for comparison with analytical techniques. A basement is introduced at a depth of 1,200 m, while the compacting field is located at a depth of 1,000 m, relatively close to the centre of compression. The elastic modulus of the subsurface down to 1,200 m is fixed at 0.5 GPa; the strength below that is varied. The results of the homogeneous Geertsma model should coincide with the new results for the profile without elasticity contrast (i.e., an elastic modulus of 0.5 GPa for the bottom layer); the Rigid Basement theory should coincide with the simulation with the rigid bottom layer. The new model has been run with eight nuclei of combined centres of compression, double forces, and centre-of-compression dipoles above the surface and around the interface, at logarithmically spaced distances of 0.4 to 6 times the distance to the centre of compaction. The total number of adjusting parameters is

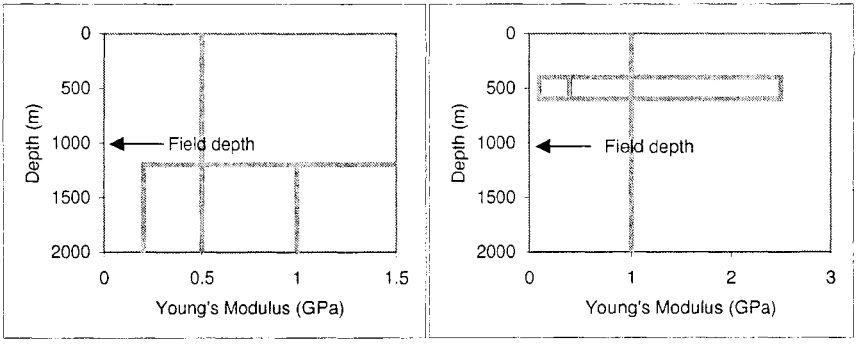



Figure 2: Test profiles for comparison with analytic models (left) and with DIANA (right; profile with 10 GPa modulus in intermediate layer not indicated in the figure).

then 72. Figure 3 shows that the agreement with the available analytical models is excellent.

Figure 3 shows further that there is already a distinct effect when the stiffness of the basement is only 1.5 times larger than the stiffness of the upper layer. It also shows that for a basement which is weaker than the overburden, the subsidence is decreased when compared to a homogeneous subsurface.

An independent measure for the accuracy can be given because the method is semi-analytic. Indeed, the deviation from the boundary conditions can be quantified. For the profile in Fig. 2, an average accuracy of less than 0.01% has been achieved.

Simulations with a finite-element simulator, DIANA, have further been used to validate the new model. This code was developed to evaluate stresses and strains in various geometries [6]. Fig. 2 (right) presents the realistic situation of a layer with deviating properties, sandwiched between the top layer of the subsurface and the layer in which the compacting field is located. The second layer is located between 400 m and 600 m deep, with the depth of the compacting field at 1,000 m. The nucleus of strain representing the compacting field is effectuated in DIANA by introducing a hollow sphere of 10 m radius in which the hydrostatic pressure is negative. The elasticity of the first and the third layer is 1 GPa; the elasticity of the intermediate layer ranges from 0.1 to 10 GPa. A rigid basement (not indicated in Fig. 2) is present at 5,000 m depth.

The resulting displacements at the surface, as calculated with DIANA and with the new method, are presented in Figure 4; the maximum displacements in the surface and the two interfaces are summarized in Table 1. It is once again clear that the agreement between DIANA and the new method

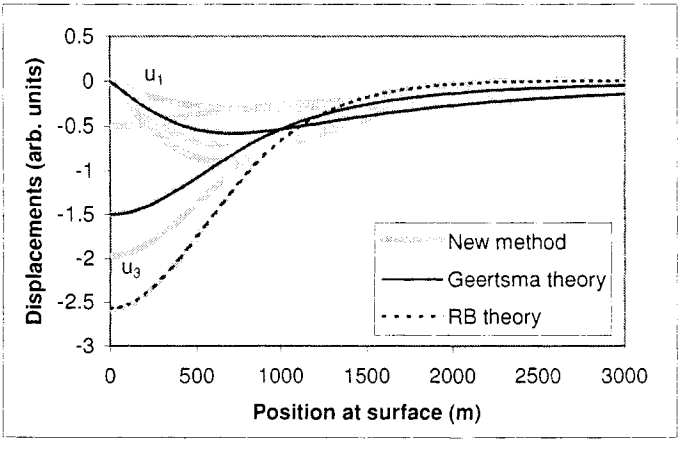



Figure 3: Comparison of the new results with available analytic methods for elasticity profiles of Fig. 2 (left). Horizontal and vertical displacements are indicated with $u_1$ and $u_3$, respectively (RB theory only provides $u_3$). The vertical scale is arbitrary since the displacement is linearly dependent on the compacting volume.

is excellent. The discrepancy between the two models at the edge of the reservoir is due to the zero-displacement boundary condition introduced in DIANA. For elasticity contrasts larger than a factor 10, the new method can become less accurate.

For a weak intermediate layer (0.1 or 0.4 GPa), the vertical displacement at the surface is larger than the reference case with equal moduli but the horizontal displacement is smaller. A wider subsidence bowl results. The weak intermediate layer allows a much larger displacement at the lowest interface, most of which disappears in the weak layer. The displacement is distributed laterally in this weak layer, resulting in the larger extension of the subsidence bowl at the second interface and at the surface, and in the related smaller horizontal displacement at the surface. For stiffer intermediate layers, both the horizontal and the vertical displacements at the surface are smaller than for the reference case. The strong layer resists displacement; consequently, the difference between the vertical displacement at the top and the bottom is relatively small.

## 5 Application to a Field Case

The new approach has been used to build a fast simulator, which can take account of a reservoir at a single depth, with a laterally varying compaction. The simulator first calculates the 'nucleus solution' for an elasticity profile of the subsurface as input and then integrates the solution over the field.

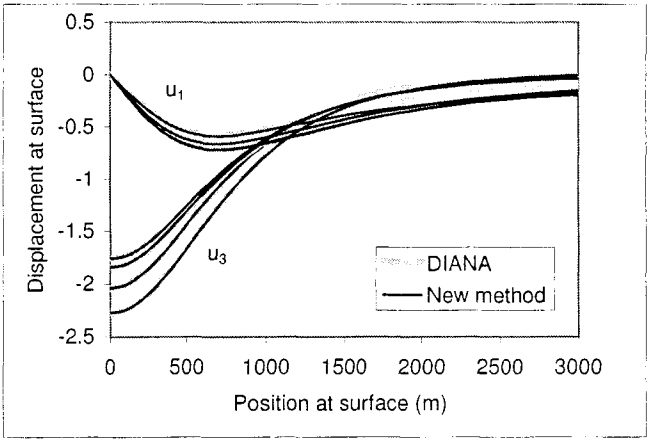



Figure 4: Validation of the new method with the finite-element simulator DIANA: effect of elasticity of an intermediate layer as indicated in Fig. 2 (right). Horizontal and vertical displacements are indicated as $u_1$ and $u_3$, respectively.

| $E$ (GPa) | DIANA | New method |
|---|---|---|
| 0.1 | 2.279 | 2.276 |
| 0.4 | 2.042 | 2.042 |
| 1.0 | 1.845 | 1.844 |
| 2.5 | 1.763 | 1.761 |
| 10 | 1.688 | 1.687 |

Table 1: Maximum vertical displacements in $\mu$m from DIANA simulations and from the new method

The simulator has turned out to be a fast method for evaluating subsidence scenarios.

The simulator has been used to assess the surface subsidence above the Ameland gas field in the northern Netherlands. The Ameland gas field is produced by NAM (Nederlandse Aardolie Maatschappij B.V.), a joint venture between Shell and Exxon. It is situated at a depth of 3,350 m, in the Upper Slochteren sandstone, below the wetlands of the Waddenzee. Having started at an initial pressure of 557 bar, the field will be depleted in 2020 with an abandonment pressure of circa 40 bar. Subsidence in this heavily monitored and well-documented field has been modelled with many different techniques over the past twenty years, resulting in a range of predictions as to what the maximum subsidence will be in the year 2020.

The new software was applied to a 2D grid of compaction coefficient,

| Prediction | Maximum subsidence (cm) | Width of subsidence bowl (km) |
|---|---|---|
| NAM 1985 | 27 | 10.2 |
| NAM 1991 | 19 | 8.9 |
| NAM 1998 | 28 | 9.1 |
| Current method | 27 | 10.4 |

Table 2: Results of NAM's predictions and results with the new method for subsidence above the Ameland gas field

pressure depletion and net reservoir height. A model with a rigid basement at 5,000 m depth and averaged geomechanical parameters for the overburden layer results in the prediction given in Table 2. Such a model results in a wider subsidence bowl than that indicated by the last NAM calculations. Therefore the geomechanical parameters of the salt layer, located between 2,100 and 3,175 m deep, have been varied. Variations give similar effects as those discussed above in connection with the DIANA simulations. The subsidence bowl continues to be somewhat wider than in the NAM simulations. We feel that the difference is due to the viscoelastic behaviour of the salt, which has not yet been modeled in the current software, limited as it is to linear elasticity. We plan to extend the software to also include linear viscoelasticity. This should fit within the framework of the theory because the extension remains linear.

## 6 Concluding remarks

The present paper presented a method to predict the surface subsidence due to the extraction of oil or gas from hydrocarbon reservoirs. For a given amount of compaction at the reservoir, it superimposes a number of solutions to the elasticity equations in such a way that the boundary conditions are approximated. Validation against available analytical expressions and against numerical approaches showed excellent performance of the new method. In addition, the accuracy of the approximation can be assessed internally for any configuration.

The method is dependent on the superposition principle and has thus been limited to linear elasticity to date. The new approach does not yet incorporate the viscoelastic behaviour of salt layers; this is scheduled for the near future. Non-linear elasticity may possibly be incorporated introducing an optimization scheme on a linearization of the equations. These extensions may be of practical interest in actual oil- and gas fields.

The new approach with the approximation of the boundary conditions makes it broader applicable than analytical approaches, while the calculation times are much smaller than for finite-element simulators. This makes it very suitable for sensitivity studies and for the evaluation of scenarios. In comparison with conventional Boundary Element Methods, the presented

method uses a least-squares approach to approximate the boundary conditions rather than the conventional approach which fulfills the boundary conditions exactly in a number of points. This gives a better approximation of the boundary conditions.

## Acknowledgement

The author wants to thank B. Orlic for carrying out the DIANA simulations.

## References

[1] A. P. E. M. Houtenbos. The quanitification of subsidence due to gas-extraction in The Netherlands. *Proc. 6th Intnl Symp. on Land Subsidence*, 1:177–189, 2000.

[2] N. B. Nagel. Ekofisk field overburden modelling. *SPE paper 47345, Eurock '98, Trondheim, Norway*, 2:177–186, 1998.

[3] J. Geertsma. A basic theory of subsidence due to reservoir compaction: The homogeneous case. *Verhandelingen Kon. Ned. Geol. Mijnbouwk. Gen.*, 28:43–62, 1973.

[4] J. Geertsma. Land subsidence above compacting oil and gas reservoirs. *J. Pet. Techn.*, pages 734–744, June 1973.

[5] G. H. C. van Opstal. The effect of base-rock rigidity on subsidence due to reservoir compaction. *Proc. 3rd Congr. Int. Soc. Rock Mech., Denver, Colorado*, 2:1102–1111, 1974.

[6] Diana's user's manual, release 7.1. *TNO Building and Construction Research*, 1999.

[7] S. L. Crouch and A. M. Starfield. *Boundary Element Methods in Solid Mechanics*. George Allen & Unwin, 1983.

[8] M. A. Biot. General theory of three-dimensional consolidation. *J. Appl. Phys.*, 12:155–164, 1941.

[9] R. D. Mindlin. Force at a point in the interior of a semi-infinite solid. *Physics*, 7:195–202, 1936.

[10] C. R. Fitts. Simple analytic functions for modeling three-dimensional flow in layered aquifers. *Wat. Res. Research*, 25(5):943–948, 1989.